Experimental Network Performance Analysis from a CBRS-based Private Mobile Network

Biswajit Kumar Dash*, Joseph A. Caezza*, and Filippo Malandra*

*Department of Electrical Engineering, State University of New York at Buffalo, NY, USA

***Abstract*—Accurately measuring propagation loss is crucial for Citizens Broadband Radio Service (CBRS) network planning, deployment, and successful spectrum sharing among CBRS users. The currently used propagation models, such as the Irregular Terrain Model (ITM) and Extended Hata (eHata) in the CBRS network, disregard significant environmental factors like foliage or clutter data, making the loss prediction unreliable. Additionally, current experimental studies on CBRS propagation are limited, with methodologies often relying on expensive measurement tools. To address these limitations, this paper proposes a CBRS network propagation framework, which includes a signal measurement system made of affordable, commercial off-the-shelf electronic devices and advanced empirical data analysis. To validate the framework, an extensive measurement campaign is conducted in a live CBRS network in Buffalo, NY. The empirical path loss results have been compared with existing analytical models, with the alpha-beta ($\alpha - \beta$) model giving the best path loss prediction. The methodology and framework presented in this paper can be applied to other network environments, helping researchers and engineers estimate network performance during the design phase, thus saving resources.**

***Index Terms*—3.5 GHz, CBRS propagation, path loss, spectrum sharing, private LTE/5G networks**

I. Introduction

Citizens Broadband Radio Service (CBRS), a 150 MHz wide band (3550-3700 MHz) within the 3.5 GHz range [1], introduces promising opportunities for users, particularly in the development of private Long Term Evolution (LTE)/Fifth Generation (5G) networks. These private networks are becoming increasingly popular solutions to provide connectivity in scenarios such as healthcare, educational facilities, smart cities, warehousing, and industrial operations. Compared to public LTE/5G, CBRS private networks offer a unique opportunity for organizations to customize their networks and rapidly roll out their communication infrastructures, reducing the reliance on telco providers. Despite the potential of CBRS for private LTE/5G networks, it introduces a set of unique challenges. For instance, setting up a private LTE/5G network can be expensive, primarily due to the required infrastructure. Improper network planning and design can further exacerbate these costs. Therefore, understanding the intended use cases and network requirements is crucial before deploying private networks. As part of this preparation, network site survey and propagation analysis form critical steps.

Unlike public LTE/5G networks, where operators purchase a licensed portion of the spectrum, thus limiting interference, the CBRS spectrum is shared. It uses a three-tier spectrum access framework [1]: i) Federal and military users have absolute priority over any other type of civil usage of this spectrum (Incumbent Access (IA) tier); ii) a portion of the spectrum can be purchased by "licensed users," typically mobile operators, that use CBRS to extend and enhance their coverage in some counties (Priority Access License (PAL) tier); iii) unlicensed General Authorized Access (GAA) users have access to all resources not currently used by IA and Priority Access (PA). Accurate measurement of propagation/path loss is vital to the success of this spectrum-sharing framework. In line with this, the CBRS standards recommend using the ITS Irregular Terrain Model (ITM) (also known as the Longley-Rice model) [2] and Extended Hata (eHata) model [3] to determine propagation for incumbent federal users and path loss calculation, respectively [4], [5]. Yet, both models have their limitations. For instance, the ITM model only considers terrain losses but not losses due to clutter like trees and leaves, while the eHata model only accounts for endpoint clutter and not losses due to foliage. Moreover, path loss characteristics, such as the path loss component and standard deviation, can differ significantly depending on the propagation environments [6]. No existing model consistently predicts path loss with minimal error across all environments. Thus, relying on a single analytical propagation model is unfeasible. Therefore, experimental data are needed to understand CBRS network propagation.

However, being a relatively new technology, only some experimental studies offer propagation data and mobile radio network planning insights for CBRS (see Section II). The measurement methodologies leveraged in these studies often rely on expensive electronic devices like spectrum analyzers (SA). Therefore, an affordable, user-friendly measurement system is paramount for advancing network planning and deployment research for the CBRS and similar technologies. To address these issues, this paper proposes a comprehensive CBRS Network Performance (CNP) framework to characterize the propagation of CBRS networks. The framework includes i) a custom-built measurement tool for signal measurement, ii) data measurement and analysis methodologies, and iii) path loss estimation and comparison with propagation models. Fig. 1 visualizes our proposed CNP framework. An extensive measurement campaign is carried out in a live CBRS network deployed in the Fruit Belt neighborhood[1], Buffalo, NY, to validate our measurement tool, and the resultant propagation loss is analyzed with existing propagation models.

The remainder of this paper is organized as follows: Section

[1]More details about the CBRS network infrastructure can be found at https://sites.google.com/view/project-overcome-buffalo.

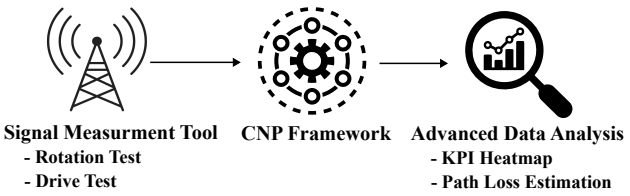

Figure 1: Architecture of the proposed CBRS Network Performance (CNP) framework.

II provides an overview of the current state of the art; Section III details the measurement system and experimental setup; Section IV discusses the measurement methodology; Section V presents the experimental results; and Section VI concludes with our research findings.

II. Related Works

While wireless communication network propagation has been extensively researched, the CBRS spectrum remains relatively under-studied due to its recent introduction by the Federal Communications Commission. Noteworthy among studies in the USA is Anderson's work on the propagation analysis of 1.7 GHz and 3.5 GHz spectrum, which introduces a novel framework integrating measurement-based techniques with a terrain and clutter model using Geographic Information Systems (GIS) datasets [7]. Another study investigates the feasibility of GAA users' coexistence using actual terrain and land cover data in two locations in the USA [8]. Outside of the USA, most propagation analyses on the 3.5 GHz spectrum band have been led by European researchers [9]–[14]. Notably, these studies have primarily focused on WiMAX systems or a continuous wave signal, overlooking the applicability of wider bandwidths, such as 150 MHz, vital for wireless systems.

The majority of existing literature generally focuses on the broad relevance of propagation models such as ECC-33, COST 231 Hata [10], Stanford University Interim (SUI) [12], Erceg [11], log-distance, Terrain Integrated Rough Earth Model (TIREM), ITM [2], and eHata [3] for network propagation and path loss estimation. However, these models have limitations. Specifically, the ECC-33 model aligns well with urban environments, whereas the SUI model fits more with suburban settings [10]. However, the Erceg model tends to underpredict path loss in both these contexts [11]. In contrast, the COST 231 Hata and SUI models overestimate path loss for rural environments [10], [12]. Moreover, as mentioned before, the ITM and eHata models ignore clutter-related losses [2] and foliage losses [3], respectively. Furthermore, the path loss characteristics, such as path loss exponent (n) and standard deviation (σ) (see equation (3)), differ significantly with propagation environments, making none of the models universally applicable to every scenario [6]. These constraints create challenges when selecting an analytical model for network planning and path loss estimation, underscoring the necessity for environment-specific validation and empirical data.

Moreover, the measurement tools in the literature rely on expensive equipment like network and spectrum analyzers and often fail to provide sufficient details for replication. Table I summarizes network types, measurement tools, and their costs from various studies. In the table, "Network Type" indicates if the experimental network is private or public. "Measurement Tool Type" denotes if the tool is custom-built or commercially available. It is important to note that most of the studies do not mention the equipment model number, so the prices in Table I are estimated based on the tool descriptions and current market rates of similar devices. Notably, these tools are expensive. Given these findings, this paper presents an affordable and replicable custom-built signal measurement tool and a signal measurement and analysis framework. Our measurement tool costs only $582, making it about 86% cheaper than the least expensive tool ($4136) used in the studies.

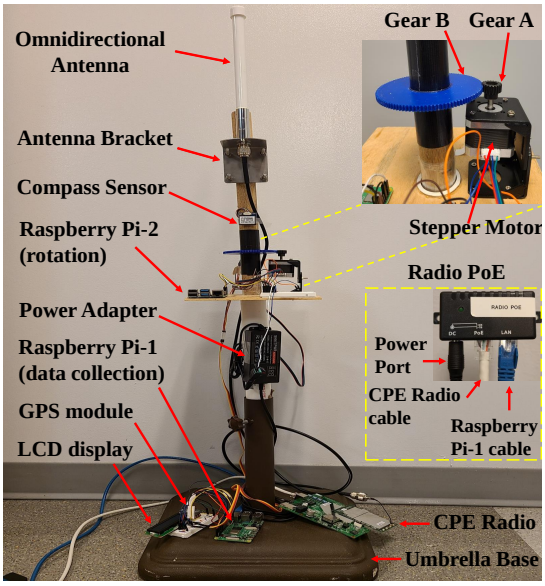

Figure 2: Measurement system consisting of measurement and rotation tools.

III. Measurement System and Experimental Setup

This section briefly describes our proposed measurement system and experimental setup.

A. Measurement System

Our custom-built measurement system depicted in Fig. 2 can be divided into two major tools: signal measurement tool and rotation tool. While the measurement tool primarily conducts signal measurements, the rotation tool rotates the antenna.

The Raspberry Pi-1 module, the principal component of our measurement tool, manages all sensor modules through Python scripts. It captures signal from the Base Station (BS) using a 7dBi M1000 omnidirectional antenna connected to a Telrad 12000 series CPE radio antenna port. Although the Telrad 12000 series antenna has four inner antennas, we use only one radio port to connect to the M1000 antenna. It is worth highlighting that we also use a 13dBi Telrad 12000 series directional antenna in our experiments. Regardless of the antenna type, the CPE radio is linked to the Raspberry Pi-1 via a radio Power over Ethernet (PoE) injector, as shown by the yellow dashed box in Fig. 2. The antenna is attached

Table I: A comparative study of network types and measurement tools in recent literature.

Source	Network Type		Measruement Tool Type		Major Components	Approx. Price($)
	Private	Public	Custom	Ready-made		
[6]	✓			✓	R&S TSMW-Z8 antenna, R&S TSMW scanner, Nemo Outdoor 5G NR	50732
[7]	✓			✓	Omnidirectional antenna, Vector Signal Analyzer	20030
[9]	✓			✓	Dipole antenna, R&S SA, Amplifier, GPS	15024
[11]	✓			✓	MA431X21 antenna, R&S FSEM30 SA, Telescopic mast, GPS	5684
[12]		✓		✓	3360 Fiberglass antenna, SA, Telescopic mast, Amplifier, GPS	4407
[13]	✓			✓	Omnidirectional antenna, SA, Pre-amplifier, GPS	4136
[14]	✓			✓	R&S TSMW WiMAX scanner, Omnidirectional antenna, GPS	11531
[15]	✓			✓	SA, Horn antenna	5257
Our work		✓	✓		M1000 Omnidirectional antenna, Telrad CPE12000SG antenna, GPS, LCD, Raspberry Pi, Compass module, Stepper motor, Umbrella base	582

to a wooden dowel rod using a 4-hole bracket. An LCD screen displays data, and a Global Positioning System (GPS) module captures time and position during signal measurement campaigns. Data is saved as a CSV file inside the Raspberry Pi-1 and offloaded to cloud storage for further use. The data can then be utilized for web application and visualization.

The rotation aspect of our measurement system is managed by a rotation tool, primarily comprising a Raspberry Pi-2 module and a stepper motor, as depicted in Fig. 2. A 100-tooth large gear is coupled with the wooden dowel rod, which rotates in sync with a 20-tooth pinion gear on a stepper motor. This creates a gear ratio of 5, which means that the dowel with the antenna turns 20% of the angle that the motor turns. Our stepper motor is configured to full steps, each equal to a 1.8°turn. Given the gear ratio, the dowel with the antenna only turns 0.36° per step, which necessitates 1000 steps for a full rotation. The rotation speed can also be configured by changing the time delay between steps. A compass sensor determines the receiver antenna's direction relative to the BS antenna. This data is used to compute the receiver antenna radiation pattern. While not explored in this work, our system can calculate the power angular spectrum and delay profile.

B. Experimental Location and Setup

An extensive measurement study is conducted in the Fruit Belt neighborhood, Buffalo, NY, to assess the propagation of a live CBRS network. The network in our research is a community CBRS network that provides wireless broadband connectivity to the Fruit Belt community [16]. It includes an LTE BS (often called eNodeB) with four directive antennas installed on the Buffalo General Medical Center (BGMC) rooftop. In our experiments, the eNodeB antenna is the transmitter, and the measurement system antenna is the receiver.

Fig. 3 visualizes the CBRS network architecture in Fruit Belt. Within this architecture, the eNodeB, represented as CBRS radio heads, connects to the LTE core network known as Evolved Packet Core (EPC) to enable the network to handle the data traffic efficiently and cost-effectively. The Spectrum Access System (SAS) manages spectrum access and sharing among CBRS users [1] and is integrated into the network EPC. The EPC is connected to a dedicated 1 Gbps optical fiber link, which is part of a Point of Presence (POP) provided by the internet service provider. To enhance security, a network firewall system is incorporated. Network switches connect the

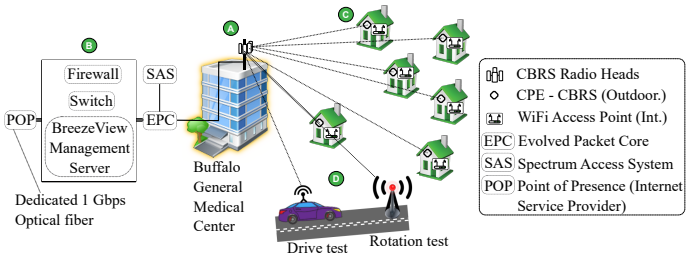

Figure 3: Architecture of the CBRS Deployment in the Fruit Belt, Buffalo, NY.

network devices, and the BreezeView Management Server performs network administrator and management tasks like performance management, real-time monitoring, reporting, and maintaining quality of service. The user end of the CBRS network is connected to the Customer Premises Equipment (CPE) installed in Fruit Belt residents' houses. Primary experimental operations in our framework, like drive and rotation tests, are also depicted in Fig. 3. Table II details the physical configuration of the eNodeB antennas, including their location, azimuth, inclination, elevation, and center frequency.

IV. Measurement Methodology

This section outlines our experimental methods and data analysis procedures, including rotation and drive tests and path loss estimation, conducted in Fruit Belt, Buffalo, NY, using our tool within an active CBRS network.

A. Rotation Test

The rotation test forms a crucial part of the methodology to compute the receiver antenna radiation pattern. The core idea is to rotate the antenna and record network KPI data. By doing this, we see how signal quality changes with antenna direction. This test helps to remove the antenna gain's effect from the received signal power, offering a more accurate representation of the network performance. The results can also help decide the best antenna placement for better network performance and user experience. Though our study does not delve into it, this test can also compute the power angular spectrum and power delay profile to characterize the multipath propagation.

The rotation tests are performed on a rooftop within Line-of-Sight (LOS) of the BS antennas. The process begins with system assembly and calibration, particularly the compass sensor,

Table II: BS antenna configurations

Configuration	BS Antenna			
	1st	2nd	3rd	4th
Latitude	42.900776	42.900788	42.900802	42.900817
Longitude	−78.865033	−78.865034	−78.865032	−78.865033
Azimuth (°)	143.5	110.5	77.5	44.5
Inclination (°)	−1	−1	−1	−1
Elevation (ft)*	115	115	115	115
Freq. (MHz)	3640	3560	3640	3560

*AGL - Above Ground Level

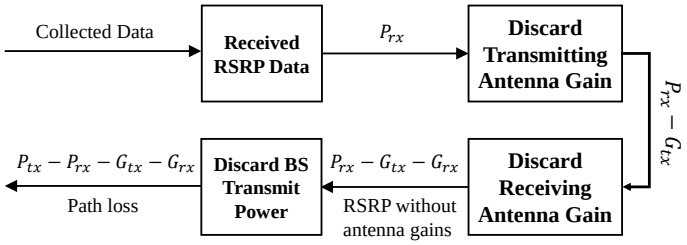

Figure 4: RSRP data post-processing to calculate path loss.

which is sensitive to metals. We validate the compass against a magnetic one to ensure accurate readings, recalibrating it as needed. Once accuracy is obtained, we rotate the receiver antenna 360 degrees, recording KPI data every 0.2 seconds. The Raspberry Pi-2-controlled stepper motor manages the rotation speed. We repeat the test multiple times, averaging results for consistency. The data is saved in a CSV file on the Raspberry Pi-1 for further analysis.

B. Drive Test

The drive test collects KPI data over a large geographic area, revealing how the network performs in different settings and distances from the BS. This helps spot coverage gaps and areas of weak and strong signals, aiding in refining the network.

For this test, the measurement antenna is mounted on the top of a measurement vehicle. We use the same assembly and calibration steps from the rotation test described in Section IV-A, except for the rotation part. The vehicle travels 10-25 mph (16-40 km/h) on Fruit Belt's public roads, and the measurement antenna records KPI data every 0.2 seconds. We track the antenna's direction and location with a compass sensor and GPS module. This helps determine the distance from the transmitter. Our test covered around 0.5 square miles (1.29 km^2) of Fruit Belt. All data gets stored for later analysis and web applications. Although omnidirectional and directional antennas are used with our tool, any antenna type should work. Fig. 3 shows our setup with a car-mounted receiver antenna representing our measurement system.

C. Path Loss Estimation

The RSRP data collected from the drive tests are post-processed to estimate path loss. Theoretically, the path loss equation can be described using the transmitted and received powers and the transmitter and receiver antenna gains. Fig. 4 presents a flowchart outlining our approach to post-process the RSRP data. Given that the collected RSRP, denoted as P_{rx}, includes gains from both the transmitter and receiver antennas, we subtract these gains from the RSRP values, hence $P_{rx} - G_{tx} - G_{rx}$. The transmitter antenna gain, G_{tx}, is obtained from the BS antenna manufacturer. We have used two receiver antennas for our tests: omnidirectional with unity gain and directional with varying gain. For the directional antenna, the gain is calculated using the rotation test mentioned in Section IV-A. We subtract the value of $P_{rx} - G_{tx} - G_{rx}$ from the transmit antenna power P_{tx} to calculate the path loss of the CBRS propagation, expressed as $P_{tx} - P_{rx} - G_{tx} - G_{rx}$. The resultant loss represents the path loss as if both the transmitting and receiving antennas had an antenna gain of 0 dBi. The path loss equation can be written as follows:

$$PL\ (dB) = P_{tx} - P_{rx} - G_{tx} - G_{rx} \tag{1}$$

where PL(dB) is the path loss in dB. P_{tx} and G_{tx} denote the transmit antenna's transmit power and gain, respectively. Similarly, P_{rx} and G_{rx} represent the receiver antenna's received power and gain, respectively.

D. Propagation Models

Propagation models like Friis Free space, log distance, alpha-beta, ITM, and eHata are commonly used to predict the propagation loss of a wireless network. Specifically, the Friis Free Space is the basic model to formulate the Free Space path loss (FSPL) and can be represented as follows.

$$FSPL(dB) = 10\log_{10}\left(\frac{4\pi d}{\lambda}\right)^2 - G_{tx} - G_{rx} \tag{2}$$

Here, λ denotes signal wavelength, and d is the distance between the transmitter and receiver, with $d \gg \lambda$. For radio waves, $\lambda = \frac{c}{f}$, with c as light speed and f as signal frequency. The log distance or close-in model extends the Friis model by adding a reference distance, d_0. The formula is:

$$[PL^{LD}(d)]\ dB = [PL(d_0)]\ dB + 10n\log_{10}(\frac{d}{d_0}) + X_\sigma \tag{3}$$

Here, $PL^{LD}(d)$ is the loss at a transmitter-receiver distance d, $PL(d_0)$ is calculated using the FSPL equation (2), n is the path loss exponent that depends on the type of environment, and X_σ accounts for shadowing effects. Typically, d_0 = 1m.

The alpha-beta ($\alpha - \beta$) model, referenced in WINNER II [17], is a regression-based model. The equation is:

$$[PL^{AB}(d)]\ dB = \alpha + 10\beta\log_{10}(d) + X_\sigma \tag{4}$$

where α and β respectively denote the intercept and slope, determined using the least squares regression on our data. In addition, the WInnForum recommends ITM [2] and eHata [3] models for CBRS networks [4], [5]. While ITM is a physics-based approach, eHata is a measurement-based empirical model. We use MATLAB to get values for these models.

In this paper, we compare our measurement-based results with the loss predicted by the models discussed above by

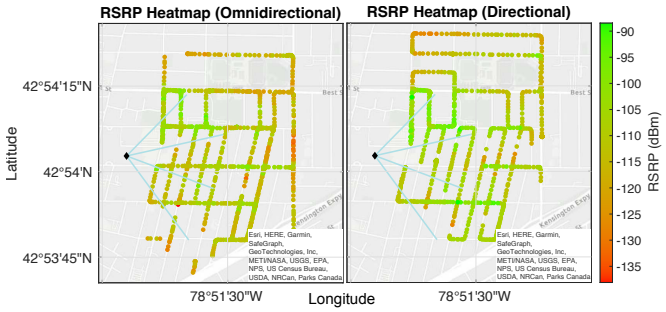

Figure 5: RSRP heatmap generated from a drive test.

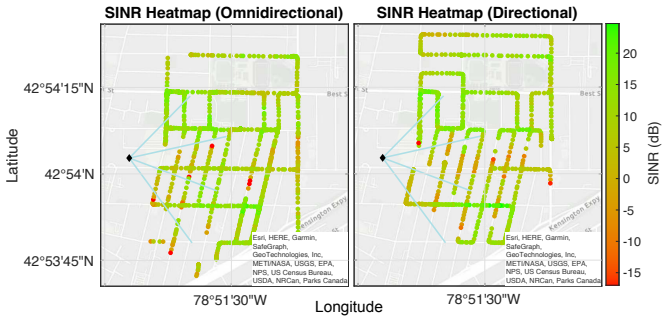

Figure 6: SINR heatmap generated from a drive test.

computing the Mean Difference (MD) and root-mean-square deviation (RMSD) using:

$$\mathrm{MD}(\hat{\theta}) = \frac{1}{N}\sum_{i=1}^{N}\hat{\theta}_i - \theta_i$$
$$\mathrm{RMSD}(\hat{\theta}) = \sqrt{\frac{\sum_{i=1}^{N}\left(\hat{\theta}_i - \theta_i\right)^2}{N}} \quad (5)$$

Here, $\hat{\theta}$ is the collected value, θ_i is the model estimated value, and N is the total number of data points.

V. Experimental Results and Discussion

The RSRP and SINR heatmaps from our drive tests with omnidirectional and directional antennas, as shown in Fig. 5 and Fig. 6, respectively, provide a comprehensive view of network performance over varying distances from the BS. The black diamond marks the BS location, the blue lines show the orientation of the four BS antennas, and the data point colors reflect RSRP quality: green for good and red for poor.

The RSRP heatmaps in Fig. 5 show that the strongest power levels are within the BS's LOS coverage. As the receiver antenna moves away from this coverage, RSRP levels drop. There are also zones on the heatmap with no RSRP, likely due to obstructions like buildings and trees. Fig. 5 also reveals that, even with the higher gain of the directional antenna, the omnidirectional antenna covers a broader area with superior power levels. This is due to the way the drive tests are conducted, where the receiver antenna is oriented toward the measurement car, not necessarily always toward the BS. As a result, the heatmap with the directive antenna sometimes shows inconsistent power levels, with patches of strong reception next to weak spots.

Fig. 6 displays SINR heatmaps from both antennas. While most of the area shows good SINR values, certain spots within the LOS exhibit poor readings, likely due to tall structures interfering with the signal. Comparing both Fig. 5 and Fig. 6, some regions, especially the lower sections, show more signal disconnections with the BS using an omnidirectional antenna than a directional one. This is likely because of the lower gain of the omnidirectional antenna than the directional one (7dBi vs 13dBi) and weak network coverage. Moreover, both figures highlight reduced network coverage between the two bottom BS antennas due to tall buildings obstructing the BS.

Fig. 7 displays measured path loss data and model predictions for the 3.5 GHz CBRS spectrum. Corresponding MD and RMSD values between actual data and model predictions are calculated using equation (5) and detailed in Table III. As seen from Fig. 7 and Table III, most models underpredict the path loss. Specifically, the ITM model, although generally aligning with data points, has a higher RMSD than the log distance and alpha-beta ($\alpha-\beta$) models. A similar underpredict is noticed for eHata but provides better prediction than the ITM model, as reflected by its lower MD and RMSD. These underpredictions can be traced back to both models' inherent limitations: the ITM model captures terrain-related losses but neglects those from buildings, foliage, and clutter, while the eHata model is better equipped to handle urban environments and building-induced losses but fails to consider specific building materials and foliage types found in our experimental settings.

Similar underpredictions are observed for the log distance model because it does not consider terrain, obstacles, and specific environmental conditions. As anticipated, the Free Space model, assuming an ideal LOS scenario, significantly underestimates path loss, yielding the highest RMSD. Conversely, the alpha-beta model displays remarkable accuracy, evidenced by a near-zero MD (-1.3509e-14 dB and 9.35e-14 dB) and a low RMSD (12.1705 dB and 12.42 dB) for omnidirectional and directional antennas, respectively. This is because the coefficients of the alpha-beta model are tuned to the specific environment using our empirical data.

It is worth highlighting here that ITM and eHata were primarily designed for large-scale broadcast scenarios featuring tall tower installations and free-space propagation within the first kilometer. These conditions do not align with our experimental scenarios, further explaining the discrepancy in results. Comparing Fig. 7(a) and (b), the path loss data shows a wider spread with the directional antenna than the omnidirectional one. While the directional antenna gain has been accounted for and subtracted from the measured RSRP data, this variability might stem from other factors, such as obstructions in the direction of the antenna during experiments.

VI. Conclusion

Accurate propagation loss measurement is vital for CBRS network planning and ensuring spectrum sharing among the tiered users. Most current models, like ITM and eHata, overlook factors like foliage and clutter, making predictions less reliable. Therefore, empirical data is essential to understand

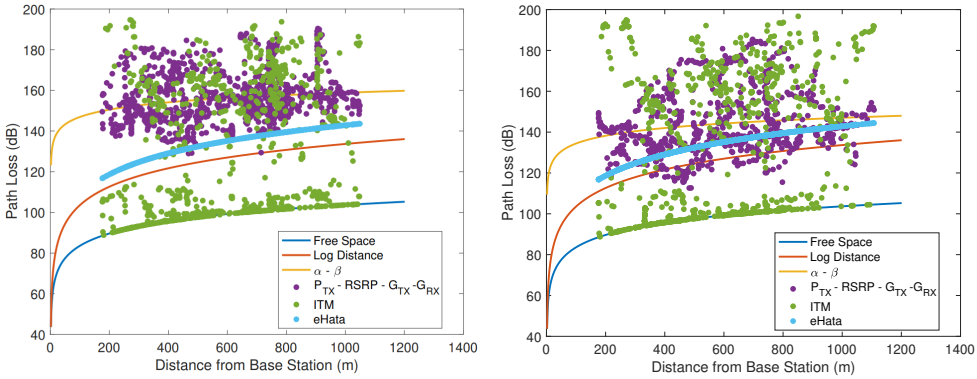

Figure 7: Measured path loss ((a) omnidirectional antenna, (b) directional antenna) compared with predicted/analytical models.

Table III: Propagation Models Vs. Experimental Results

Antenna Type	Omnidirectional		Directional	
Model	**Mean (dB)**	**RMS (dB)**	**Mean (dB)**	**RMS (dB)**
ITM	-29.19	43.86	-10.04	41.09
eHata	-21.66	25.15	-9.89	17.65
Log Distance	-29.69	32.24	-17.87	22.95
α–β	-1.35e-14	12.17	9.35e-14	12.42
Free Space	-57.21	58.50	-45.27	47.41

the propagation of the CBRS network. However, as CBRS is a new technology, there is a lack of experimental data, and studies often depend on expensive measurement tools.

This paper presents a CNP framework to characterize the CBRS network propagation. An affordable measurement system is built using COTS devices, such as Raspberry Pi, a stepper motor, and GPS modules. Extensive measurement campaigns are carried out in the Fruit Belt neighborhood, Buffalo, under a live CBRS network, and the path loss values are computed. We observe consistent underpredictions from standard models compared to our experimental path loss results, where the alpha-beta model performs best. Importantly, our proposed CNP framework is versatile and applicable across various wireless systems and experimental environments.

Acknowledgement

The authors would like to thank the Center of Excellence in Materials Informatics (CMI) at the University of Buffalo and Integrated Systems for funding this project.

References

[1] Federal Communications Commission (FCC), "3.5 GHz Band Overview," August, 2022. [Online]. Available: https://www.fcc.gov/wireless/bureau-divisions/mobility-division/35-ghz-band/35-ghz-band-overview

[2] A. G. Longley and P. L. Rice, *Prediction of tropospheric radio transmission loss over irregular terrain: A computer method-1968*. Institute for Telecommunication Sciences, 1968, vol. 67.

[3] E. F. Drocella Jr., J. C. Richards, R. L. Sole, F. Najmy, A. Lundy, and P. M. McKenna, "3.5 GHz exclusion zone analyses and methodology," *NTIA Tech. Rep. 15-517*, June, 2015. [Online]. Available: http://www.its.bldrdoc.gov/publications/2805.aspx

[4] Wireless innovation Forum (WInnForum), "Requirements for commercial operation in the U.S. 3550–3700 MHz citizens broadband radio service band," December, 2022. [Online]. Available: https://winnf.memberclicks.net/assets/CBRS/WINNF-TS-0112.pdf

[5] Federal Communications Commission (FCC), "Amendment of the Commission's Rules with Regard to Commercial Operations in the 3550-3650 MHz Band," *document FCC 15-47*, April, 2015. [Online]. Available: https://docs.fcc.gov/public/attachments/FCC-15-47A1.pdf

[6] A. Schumacher, R. Merz, and A. Burg, "3.5 GHz Coverage Assessment with a 5G Testbed," in *2019 IEEE 89th Vehicular Technology Conference (VTC2019-Spring)*, 2019, pp. 1–6.

[7] C. R. Anderson, "An Integrated Terrain and Clutter Propagation Model for 1.7 GHz and 3.5 GHz Spectrum Sharing," *IEEE Transactions on Antennas and Propagation*, vol. 70, no. 7, pp. 5804–5818, 2022.

[8] W. Gao and A. Sahoo, "Performance Study of a GAA-GAA Coexistence Scheme in the CBRS Band," in *2019 IEEE International Symposium on Dynamic Spectrum Access Networks (DySPAN)*, 2019, pp. 1–10.

[9] M. Walden and F. Rowsell, "Urban propagation measurements and statistical path loss model at 3.5 GHz," in *2005 IEEE Antennas and Propagation Society International Symposium*, vol. 1A, 2005, pp. 363–366 Vol. 1A.

[10] V. Abhayawardhana, I. Wassell, D. Crosby, M. Sellars, and M. Brown, "Comparison of empirical propagation path loss models for fixed wireless access systems," in *2005 IEEE 61st Vehicular Technology Conference*, vol. 1, 2005, pp. 73–77 Vol. 1.

[11] W. Joseph, L. Roelens, and L. Martens, "Path Loss Model for Wireless Applications at 3500 MHz," in *2006 IEEE Antennas and Propagation Society International Symposium*, 2006, pp. 4751–4754.

[12] P. Imperatore, E. Salvadori, and I. Chlamtac, "Path Loss Measurements at 3.5 GHz: A Trial Test WiMAX Based in Rural Environment," in *2007 3rd International Conference on Testbeds and Research Infrastructure for the Development of Networks and Communities*, 2007, pp. 1–8.

[13] S. Kun, W. Ping, and L. Yingze, "Path loss models for suburban scenario at 2.3GHz, 2.6GHz and 3.5GHz," in *2008 8th International Symposium on Antennas, Propagation and EM Theory*, 2008, pp. 438–441.

[14] K. L. Chee, S. A. Torrico, and T. Kurner, "Foliage Attenuation Over Mixed Terrains in Rural Areas for Broadband Wireless Access at 3.5 GHz," *IEEE Transactions on Antennas and Propagation*, vol. 59, no. 7, pp. 2698–2706, 2011.

[15] K. Tateishi, D. Kunta, A. Harada, Y. Kishryama, S. Parkvall, E. Dahlman, and J. Furuskog, "Field experiments on 5G radio access using 15-GHz band in outdoor small cell environment," in *2015 IEEE 26th Annual International Symposium on Personal, Indoor, and Mobile Radio Communications (PIMRC)*, 2015, pp. 851–855.

[16] F. Malandra, M. Silbey, R. Alvarez, B. Cacace, and T. Hege, "Community CBRS Networks - What You Need to Know," in *2022 IEEE Future Networks World Forum (FNWF)*, 2022, pp. 228–231.

[17] P. Kyösti, J. Meinilä, L. Hentila, X. Zhao, T. Jämsä, C. Schneider, M. Narandzic, M. Milojević, A. Hong, J. Ylitalo, V.-M. Holappa, M. Alatossava, R. Bultitude, Y. Jong, and T. Rautiainen, "WINNER II channel models," *IST-4-027756 WINNER II D1.1.2 V1.2*, 02 2008.